

CONVERGENCE CHARACTERISTICS OF MULTIGRID SOLUTIONS OF NON-ISOTHERMAL LAMINAR FLOWS IN POROUS MEDIA

Maximilian S. Mesquita

Marcelo J. S. De-Lemos *

Departamento de Energia – IEME

Instituto Tecnológico de Aeronáutica – ITA

12228-900 - São José dos Campos - SP – Brazil

* Corresponding author. E-mail: delemos@mec.ita.cta.br

Abstract. This work investigates the efficiency of the Multigrid numerical method when applied to solve the temperature field in a tank filled with a porous substrate. The numerical method includes finite volume discretization with the flux blended deferred correction scheme on structure orthogonal regular meshes. The correction storage (CS). Multigrid algorithm performance is compared for different values of porosity and permeability. Up to four grid for both W- and V-cycles are considered. Results indicate that also for flow in porous media there are advantages in using more than one computational grid when numerically solving the governing equations.

Keywords. Numerical Method, Multigrid, Laminar Flow, Porous media

1. Introduction

In most iterative numerical solutions, convergence rates of single-grid calculations are greatest in the beginning of the process, slowing down as the iterative process goes on. Effects like those get more pronounced as the grid becomes finer. Large grid sizes, however, are often needed when resolving small recirculating regions or detecting high heat transfer spots. The reason for this hard-to-converge behavior is that iterative methods can efficiently smooth out only those Fourier error components of wavelengths smaller than or comparable to the grid size. In contrast, Multigrid methods aim to cover a broader range of wavelengths through relaxation on more than one grid.

The number of iterations and convergence criterion in each step along consecutive grid levels visited by the algorithm determines the cycling strategy, usually a V- or W-cycle. Within each cycle, the intermediate solution is relaxed before (pre-) and after (post-smoothing) the transportation of values to coarser (restriction) or to finer (prolongation) grids (Brandt (1977), Stüben & Trottenberg (1982), Hackbusch (1985)).

Accordingly, Multigrid methods can be roughly classified into two major categories. In the CS formulation algebraic equations are solved for the corrections of the variables whereas, in the full approximation storage (FAS) scheme, the variables themselves are handled in all grid levels. It has been pointed out in the literature that the application of the CS formulation is recommended for the solution of linear problems being the FAS formulation more suitable to non-linear cases (Brandt (1977), Stüben & Trottenberg (1982), Hackbusch (1985)). An exception to this rule seems to be the work of Jiang, et al (1991), who reported predictions for the Navier-Stokes equations successfully applying the Multigrid CS formulation. In the literature, however, not too many attempts in solving non-linear problems with Multigrid linear operators are found.

Acknowledging the advantages of using multiple grids Rabi & de Lemos (1998a, 2001, 2003) presented numerical computations applying this technique to recirculating flows in several geometries of engineering interest. There, the correction storage (CS) formulation was applied to non-linear problems. Later, Rabi & de Lemos (1998b, analyzed the effect of Peclet number and the use of different solution cycles when solving the temperature field within flows with a given velocity distribution. In all those cases, the advantages in using more than one grid in iterative solution was confirmed, furthermore, de Lemos & Mesquita (1999), introduced the solution of the energy equation in their Multigrid algorithm. Temperature distribution was calculated solving the whole equation set together with the flow field as well as uncoupling the momentum and energy equations. A study on optimal relaxation parameters was there reported.

More recently Mesquita & de Lemos (2000a-b, 2003) analyzed the influence of the increase of points of the mesh and optimal values of the parameters of the Multigrid cycle for different geometries.

The present contribution extends the early work on CS Multigrid methods to the solution of temperature field in porous media. More specifically, steady-state laminar flow in a tank totally filled with a porous material is calculated with up to 4 grids. A schematic of such configurations is show in Figure 1.

2. Governant Equations and Numerics

A macroscopic form of the governing equations is obtained by taking the volumetric average of the entire equation set. In this development, the porous medium is considered to be rigid, undeformable and saturated by an incompressible fluid.

The microscopic continuity equation for the fluid phase is given by:

$$\nabla \cdot \mathbf{u} = 0 \quad (1)$$

Applying the volume-average operator to equation (1), one has (see Pedras & de Lemos (2001) for details),

$$\nabla \cdot \mathbf{u}_D = 0 \quad (2)$$

The Dupuit-Forchheimer relationship, $\mathbf{u}_D = \phi \langle \mathbf{u} \rangle^i$, has been used where the operator “ $\langle \rangle$ ” identifies the intrinsic (liquid volume based) average of \mathbf{u}_D [Gray & Lee (1977)]. Equation 2 represents the macroscopic continuity equation for an incompressible fluid in a rigid porous medium.

The microscopic Navier-Stokes equation for an incompressible fluid with constant properties can be written as,

$$\rho \nabla(\mathbf{u}\mathbf{u}) = -\nabla p + \mu \nabla^2 \mathbf{u} \quad (3)$$

Hsu & Cheng (1990) have applied the volume averaging procedure to equation 3 obtaining,

$$\nabla(\rho \phi \langle \mathbf{u}\mathbf{u} \rangle^i) = -\nabla(\phi \langle p \rangle^i) + \mu \nabla^2(\phi \cdot \langle \mathbf{u} \rangle^i) + \mathbf{R} \quad (4)$$

where

$$\mathbf{R} = \frac{\mu}{\Delta V} \int_{A_i} n(\nabla \cdot \mathbf{u}) dS - \frac{1}{\Delta V} \int n p dS \quad (5)$$

The term \mathbf{R} represents the total drag per unit volume acting on the fluid by the action of the porous structure. A common model for it is known as the Darcy-Forchheimer extended model and is given by:

$$\mathbf{R} = - \left[\frac{\mu \phi}{K} \mathbf{u}_D + \frac{c_F \phi \rho |\mathbf{u}_D| \mathbf{u}_D}{\sqrt{K}} \right] \quad (6)$$

where the constant c_F is known in the literature as the non-linear Forchheimer coefficient. Then, making use of the expression, $\mathbf{u}_D = \phi \langle \mathbf{u} \rangle^i$, equation 4 can be rewritten as,

$$\left[\nabla \left(\frac{\mathbf{u}_D \mathbf{u}_D}{\phi} \right) \right] = -\nabla(\phi \langle p \rangle^i) + \mu \nabla^2 \mathbf{u}_D - \left[\frac{\mu \phi}{K} \mathbf{u}_D + \frac{c_F \phi \rho |\mathbf{u}_D| \mathbf{u}_D}{\sqrt{K}} \right] \quad (7)$$

The microscopic energy equation for an incompressible fluid with constant properties can be written as,

$$\rho \nabla(\mathbf{u}T) = \frac{\mu}{Pr} \nabla^2 T \quad (8)$$

Rocamora & De Lemos (2000) have applied the volume averaging procedure using the concept of double decomposition concept to equation 8 obtaining, the macroscopic energy equations for an incompressible flow in a rigid, homogeneous and saturated porous medium can be written as:

$$(\rho c_p)_f \nabla \left[\left[k_f \phi + k_s (1 - \phi) \right] \nabla \langle T \rangle^i \right] \quad (9)$$

The thermal conductivity for the fluid and solid are labeled k_f and k_s respectively. Finally, c_p is the specific heat and ϕ is the porosity, K is the permeability and c_F is the Forchheimer coefficient.

2.1. Numerical Model

The solution domain is divide into a number of rectangular control volumes (CV), resulting in a structure orthogonal non-uniform mesh. Grid points are located according to a *cell-centered* scheme and velocities are store in a *collocated* arrangement (Patankar (1980)). A typical CV with its main dimensions and internodal distances is sketched in Figure 2 Writing equations (2)-(4) in terms of a general form ϕ

$$\frac{\partial}{\partial x} \left(\rho U \phi - \Gamma_\phi \frac{\partial \phi}{\partial x} \right) + \frac{\partial}{\partial y} \left(\rho V \phi - \Gamma_\phi \frac{\partial \phi}{\partial y} \right) = S_\phi \quad (10)$$

where ϕ stands for U, V, and P. Integrating the equation 10 over the control volume of Figure 2,

$$\int_{\delta v} \left[\frac{\partial}{\partial x} (\rho U \phi) + \frac{\partial}{\partial y} (\rho V \phi) \right] dv = \int_{\delta v} \left[\frac{\partial}{\partial x} \left(\Gamma_\phi \frac{\partial \phi}{\partial x} \right) + \frac{\partial}{\partial y} \left(\Gamma_\phi \frac{\partial \phi}{\partial y} \right) \right] dv + \int_{\delta v} S_\phi dv \quad (11)$$

Integration of the three terms in 11, namely: convection, diffusion and source, lead to a set of algebraic equations. These practices are described elsewhere (e.g. Patankar (1980)) and for this reason they not repeated here. In summary,

convective terms are discretized using the upwind differencing scheme (UDS), diffusive fluxes make use of the central differencing scheme.

Substitution of all approximate expressions for interface values and gradients into the integrated transport equation 11, gives the final discretization equation for grid node P

$$a_P \phi_P = a_E \phi_E + a_W \phi_W + a_N \phi_N + a_S \phi_S + b \quad (12)$$

with the east face coefficient, for example, being define as

$$a_E = \max[-C_e, 0] + D_e \quad (13)$$

In (13) $D_e = \mu_e \delta_y / \Delta x_e$ and $C_e = (\rho U)_e \delta_y$ are the diffusive and convective fluxes at the CV east face, respectively.

2.2. Multigrid Technique

Assembling equation 12 for each control volume of Figure 1 in the domain of Figure 2 defines a linear algebraic equation system of the form,

$$A_k T_k = b_k \quad (14)$$

where A_k is the *matrix of coefficients*, T_k is the *vector of unknowns* and b_k is the vector accommodating source and extra terms. Subscript “k” refers to the grid level, with k=1 corresponding to the coarsest grid and k=M to the finest mesh. defined as

As mentioned, Multigrid is here implemented in a *correction storage* formulation (CS) in which one seeks coarse grid approximations for the *correction* defined as $\delta_k = T_k - T_k^*$ where T_k^* is an *intermediate value* resulting from a small number of iterations applied to (14). For a linear problem, one shows that δ_k is the solution of (Brandt (1977), Stüben & Trottenberg (1982), Hackbusch (1985)),

$$A_k \delta_k = r_k \quad (15)$$

where the *residue* is defined as

$$r_k = b_k - A_k T_k^* \quad (16)$$

Eq. (10) can be approximated by means of a coarse-grid equation,

$$A_{k-1} \cdot \delta_{k-1} = r_{k-1} \quad (17)$$

with the *restriction operator* I_k^{k-1} used to obtain

$$r_{k-1} = I_k^{k-1} r_k \quad (18)$$

The residue restriction is accomplished by summing up the residues corresponding to the four fine grid control volumes that compose the coarse grid cell. Thus, equation 18 can be rewritten as,

$$r_{k-1}^{IJ} = r_k^{IJ} + r_k^{j+1} + r_k^{i+1j} + r_k^{i+1j+1} \quad (19)$$

Diffusive and convection coefficients in matrix A_k need also to be evaluated when changing grid level. Diffusive terms are recalculated since they depend upon neighbor grid node distances whereas coarse grid mass fluxes (*convective terms*) are simply added up at control volume faces. This operation, is commonly found in the literature (Peric, et al (1989), Hortmann et al (1990)).

Once the coarse grid approximation for the correction δ_{k-1} has been calculated, the *prolongation* operator I_{k-1}^k takes it back to the fine grid as

$$\delta_k = I_{k-1}^k \delta_{k-1} \quad (20)$$

In order to update the intermediate value

$$T_k = T_k^* + \delta_k \quad (21)$$

Figure 3 illustrates a 4-grid iteration scheme for both the *V*- and *W*-cycles where the different operations are: *s*=smoothing, *r*=restriction, *cg*=coarsest grid iteration and *p*=prolongation. Also, the number of domain sweeps before and after grid change is denoted by v^{pre} and v^{post} , respectively. In addition, at the coarsest k level ($k=1$), the grid is swept v^{cg} times by the error smoothing operator

3. Results and Discussion

The computer code developed was run on a IBM PC machine with a dual processor Pentium III 1.0 GHz. Grid independence studies were conducted such that the solutions presented herein are essentially grid independent. For both *V*- cycles, pre- and post-smoothing iterations were accomplished via the Gauss-Seidel algorithm while, at the coarsest-grid, the TDMA method has been applied (Patankar (1980)). Also, the geometry of Figure 1 was run with the finest grid having sizes of 66x66 grid points.

With the aim of checking the accuracy of the numerical solution, after implementation of porous media model, the limiting case of flow in clear fluid was simulated by setting $\phi = 0.998$, $K = 1 \times 10^{10} \text{ m}^2$ and $c_F = 0$. Figure 4 shows velocity profiles at the exit of the tank. The figure indicates that the solution with the porous model reproduces the clear flow situation when appropriate parameters are used.

Residues. The residue is normalized and calculated according to

$$R_U = \sqrt{\sum_{ij} (R_{ij})^2} \quad (22)$$

with $R_{ij} = a_p U_p - (\sum_{nb} a_{nb} U_{nb})$ where subscript *ij* identifies a given control volume on the finest grid and *nb* refers to its neighboring control volumes.

Figures 5 and 6 shows residue history for the heated tank filled with porous material case following the two cycles picture on Figure 3, namely the *V*- and *W*- Cycles. The solutions follows a simultaneous approach in the sense that the temperature is always relaxed after the flow field, within the multigrid cycle. One can readily notice for both cycles that for $Re_{in} = 300$, regardless of the number of grids used, faster solutions are obtained. In this case, relative importance of diffusion terms favors the stability of the system of equations. Also interesting to note is that for the *V*-cycle (Figure 5) the computational effort related to value transfers among too many grids became relevant. Using *W*-cycle (6) seems to bring more savings to the iterative simultaneous solution procedure. When recalling the nature of the *W* – cycle in comparison with the *V* – strategy (Figure 3), one can see that the number of grids transfer per cycle is less in the former algorithm. In addition, the more work done in the lower frequency range spectrum with the *W*- cycle contributes for a faster overall solution. The effect of medium permeability on residue history for the energy equation is shown in Figure 7. Higher values of K require less computational effort to achieve convergence. This effect seems to be associated with the fact that the higher the permeability, more intensive are convection currents, leading, ultimately, to more convective-dominated situations.

The effect of the medium porosity on the residue reduction rate of the U is presented in Figures 8 using the multigrid methodologies. The higher the porosity, the closer the flow is to unobstructed situation which, in turn, makes it harder for the algebraic equations to converge.

In the works of Rabi & de Lemos (1998b, 2001,2003) and Mesquita & de Lemos (2000a-b, 2003), a study was carried out to investigate optimal values for the parameters v^{pre} , v^{post} and v^{cg} . Since the intermediate solutions, before and after grid changes, are not fully solved but are rather relaxed v^{pre} and v^{post} times, a question about their optimal values for increasing overall algorithm performance arises. Or say, as restriction and prolongation operations may also introduce imprecision to values being transferred, one should expect the computational effort to be sensitive to the number of smoothing sweeps. In the other words, once the intermediate numerical solution has been relaxed a number of times removing errors introduced by transfer operators and further reducing the residue, it is of no use to keep iterating at a certain grid level. The next figures help to analyze the existence of such optimal intermediate smoothing.

For a fixed number of sweeps at the coarse grid Figure 9 reproduces the necessary time to convergence when the number of pre- and post-smoothing iterations was allowed to vary, keeping $v^{pre} = v^{post}$. Figure 9 show results for the heated tank filled within porous material case with $v^{cg} = 5$. In Figure one can see that more than one sweep for relaxing the intermediate solution, before and after grid change brings advantage to the algorithm performance. Consequently, further relaxation past this limit unnecessarily increases the computational effort, this effect is more pronounced for higher porosity.

In Figure 10 the number of pre- and post-smoothing iterations was fixed conform was indicated in legend, whereas the number of coarsest-grid sweeps v^{cg} was free to vary. For the present case, an optimum situation can be clearly identified for lower porosities ($\phi = 0.20, 0.40$ and 0.60). For higher porosities ($\phi = 0.80$ and 0.95) no minimum value for the number of sweeps at coarsest grid were detected. Only one pass through the domain is enough for obtaining best results.

Ultimately, both Figures 9 and 10 suggest a delicate balance between all parameters involved when minimum CPU consumption is sought. Most often, optimal parameters can not be easily determined *a priori* and adaptive strategies have been proposed in the literature. Generally, the ratio of residues after two successive sweeps is monitored and used as a criterion for switching grids. Hortmann *et al* (1990) points out that this practice is preferred for single equation systems but, when solving the full equation set as done here, most works in the literature specify a fixed number of sweeps, as in the cases here reported Sathyamurthy & Patankar (1994), Hutchinson *et al* (1988).

4. Conclusions

The Multigrid method has been implemented in a correction storage manner to numerically solve a two-dimensional steady-state conduction-convection in porous medium problem. Structured, orthogonal and regular meshes were used and discretized equations were obtained through a finite volume formulation. The overall algorithm performance was compared for different values of the porosities and permeability, for distinct cycles, for different number of intermediate solution sweeps and coarsest-grid iterations.

Results proved the superiority of the multigrid method against single grid calculations. For the cases here studied, they indicated that decreasing the value of K tends to increase the required computational effort and that increasing the value of ϕ tends to increase the computational effort. These behaviors, however, may not be general and may depend on additional characteristics of the flow in question.

5. Acknowledgement

The authors are thankful to CNPq, Brazil, for their financial support during the preparation of this work

6. References

- Brandt, A., 1977, Multi-Level Adaptive Solutions To Boundary-Value Problems, *Math. Comp.*, Vol. 31, No. 138, Pp. 333-390.
- de Lemos, M.J.S., Mesquita, M.S., 1999, Multigrid Numerical Solutions Of Non-Isothermal Laminar Recirculating Flows, *Applications Of Computational Heat Transfer*, ASME-HTD-Vol. 364-3, ISSN: 0272-5673, ISBN: 0-7918-1656-7, Ed..L.C. White, Pg. 323-330.
- Gray, W.G., Lee, P.C.Y., 1977, On the Theorems for Local Volume Averaging of Multiphase System, *Int. J. Multiphase Flow*, vol. 3, pp. 333-340.
- Hackbusch, W., 1985, *Multigrid Methods And Applications*, Springer-Verlag, Berlin.
- Hortmann, M., Peric, M., Scheuerer, G., 1990, Finite Volume Multigrid Prediction Of Laminar Convection: Benchmark Solutions, *Int. J. Num. Meth. Fluids*, Vol. 11, Pp. 189-207.
- Hsu, C.T., Cheng, P., 1990, Thermal dispersion in a porous medium, *Int. J. Heat Mass Transfer*, vol. 33, pp. 1587-1597.
- Hutchinson, B.R., Galpin, P.F., Raithby, G.D., 1988, Application Of Additive Correction Multigrid To The Coupled Fluid Flow Equations, *Num. Heat Transfer*, Vol. 13, Pp. 133-147.
- Jiang, Y., Chen, C.P., Tucker, P.K., 1991, Multigrid Solutions Of Unsteady Navier-Stokes Equations Using A Pressure Method, *Num. Heat Transfer - Part A*, Vol. 20, Pp. 81-93.
- Mesquita, M.S., de Lemos, M.J.S., 2000a, Numerical Solution Of Non-Isothermal Laminar Recirculating Flows Using The Multigrid Method, Encit 2000, Porto Alegre, RS, Brazil, 2000.
- Mesquita, M.S., de Lemos, M.J.S., 2000b, Multigrid Numerical Solutions Of Laminar Back Step Flow, Congresso Nacional De Engenharia Mecânica, Natal, Rn, Brazil, 2000.
- Mesquita, M.S., de Lemos, M.J.S., 2003, Optimal Multigrid Solutions Of Two Dimensional Convection-Conduction Problems, *Applied Mathematics and Computation* (submitted).
- Patankar S.V., Spalding D. B., 1972, A Calculation Procedure For Heat, Mass And Momentum Transfer In Three-Dimensional Parabolic Flows, *Int. J. Heat Mass Transfer*, Vol. 15, Pp.1787-1806.
- Patankar, S.V., 1980, *Numerical Heat Transfer And Fluid Flow*, Mc-Graw Hill.
- Pedras, M.H.J., de Lemos, M.J.S., 2000a, On the Definition of Turbulent Kinetic Energy for Flow in Porous Media, *Int. Comm. In Heat & Mass Transfer*, vol. 27 (2), pp. 211-220.

- Pedras, M.H.J., de Lemos, M.J.S., 2001, Macroscopic Turbulence Modeling For Incompressible Flow Through Undeformable Porous Media, *Int. J. Heat Mass Transfer*, Vol. 44(6), pp. 1081-1093.
- Peric M., R ger M., Scheurer G., 1989, A Finite Volume Multigrid Method For Predicting Periodically Fully Developed Flow, *Int. J. Num. Fluids*, Vol. 18, Pp.843-852.
- Peric, M., R ger, M., Scheuerer, G., 1989, A Finite Volume Multigrid Method For Calculating Turbulent Flows, In: *Seventh Symposium On Turbulent Shear Flows*, Pp. 7.3.1-7.3.6, Stanford University.
- Rabi, J.A., de Lemos, M.J.S., 1998a, Multigrid Numerical Solution Of Incompressible Laminar Recirculating Flows, Encit98- Proc. Of 7th Braz. Cong. Eng. Th. Sci., Vol. 2, Pp. 915-920, Rio De Janeiro, RJ, Nov. 3-6.
- Rabi, J.A., de Lemos, M.J.S., 1998b, The Effects Of Peclet Number And Cycling Strategy On Multigrid Numerical Solutions Of Convective-Conductive Problems, *7th AIAA/ASME Jnt Thermcs & HT Conf*, **Paper AIAA-98-2584**, Albuquerque, New Mexico, USA, June 15-18.
- Rabi, J.A., de Lemos, M.J.S., 2001, Optimization of Convergence Acceleration in Multigrid Numerical Solutions of Conductive-Conductive Problems, *Applied Mathematics and Computation*, vol. 124, n. 2, pp.215-226.
- Rabi, J.A., de Lemos, M.J.S., 2003, Multigrid correction-storage formulation applied to the numerical solution of incompressible laminar recirculating flows, *Applied Mathematical Modelling* (accepted, in press).
- Raithby, G.D., Torrance, K.E., 1974, Upstream-Weighted Differencing Schemes And Their Application To Elliptic Problems Involving Fluid Flow, *Comp. & Fluids*, Vol. 2, Pp. 191-206.
- Rocamora, F. D. Jr., De Lemos, M.J.S., Analysis of Convective Heat Transfer for Turbulent Flow in Saturaded Porous Media, *Int. Comm. Heat Mass Transfer*, Vol.27, No.6, pp.825-834, 2000.
- Sathyamurthy, P.S., Patankar, S.V., 1994, Block-Correction-Based Multigrid Method For Fluid Flow Problems, *Numerical Heat Transfer - Part B*, Vol. 25, Pp. 375-394.
- St ben, K., Trottenberg, U., 1982, Multigrid Methods, In *Lect. Notes Math.*, Vol. 960, Pp. 1-76, Berlin
- Thompson, M.C., Ferziger, J.H., 1989, An Adaptive Multigrid Technique For The Incompressible Navier-Stokes Equations, *J. Comp. Phys.*, Vol. 82, Pp. 94-121.
- Vanka, S.P. 1986, Block-Implicit Multigrid Calculation Of Two-Dimensional Recirculating Flows, *Comp. Meth. Appl. Mech. Eng.*, Vol. 86, Pp. 29-48.

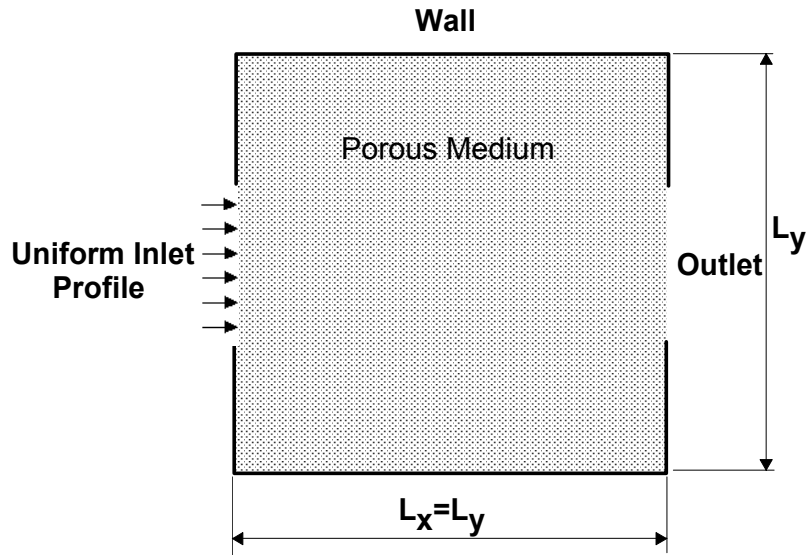


Figure 1 - Geometry and boundary conditions

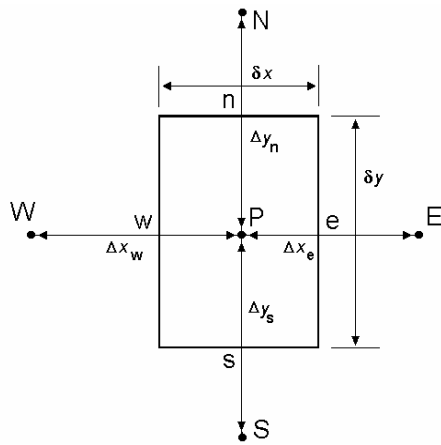


Figure 2 - Control Volume for discretization

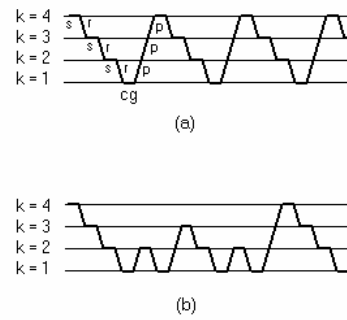


Figure 3 - Sequence of Operation in a 4-grid iteration
(a)V-cycle, (b)W-cycle

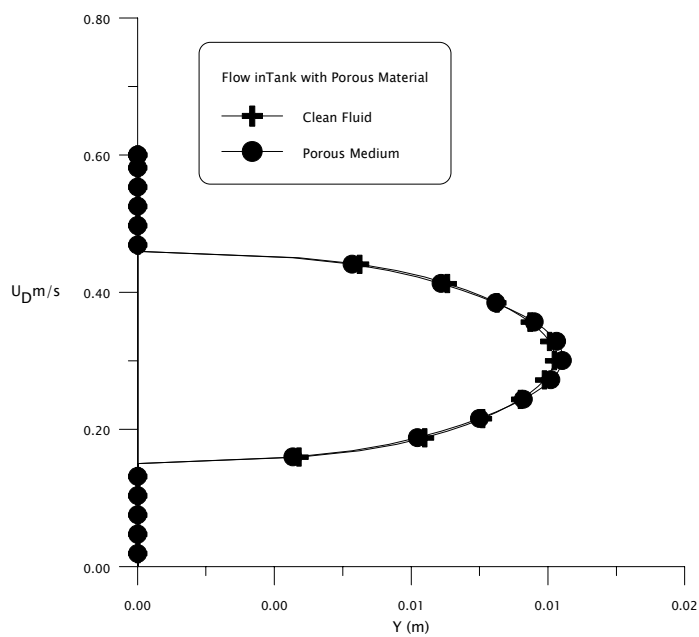


Figure 4 - Velocity profiles at the exit of a tank for porous medium with $cF=0.0$, $\square=0.998$ and $K=1 \times 10^{10} \text{ m}^2$

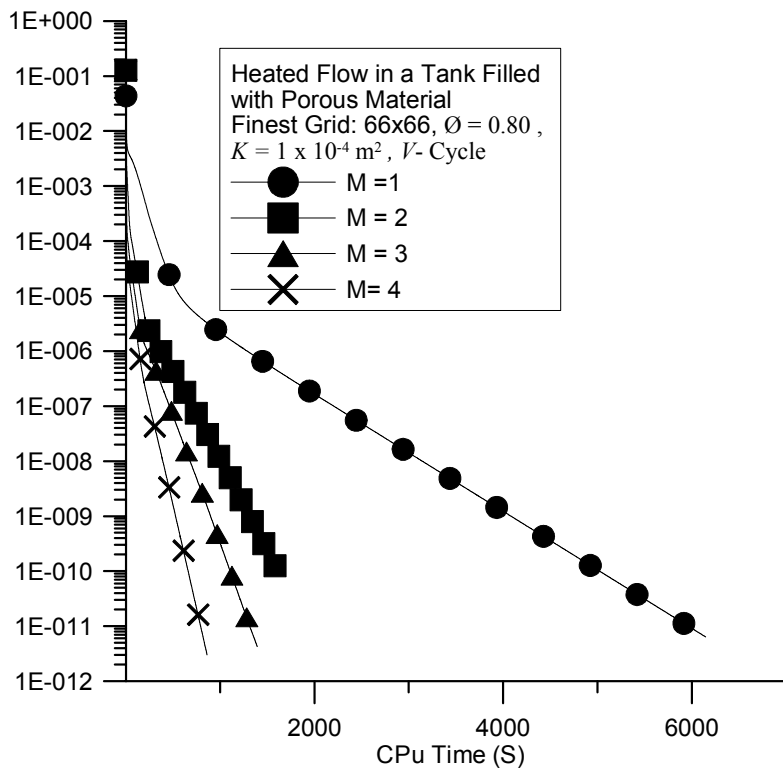


Figure 5 – Residue history for different number of grids, $Re_{in} = 300$, *V*-Cycle.

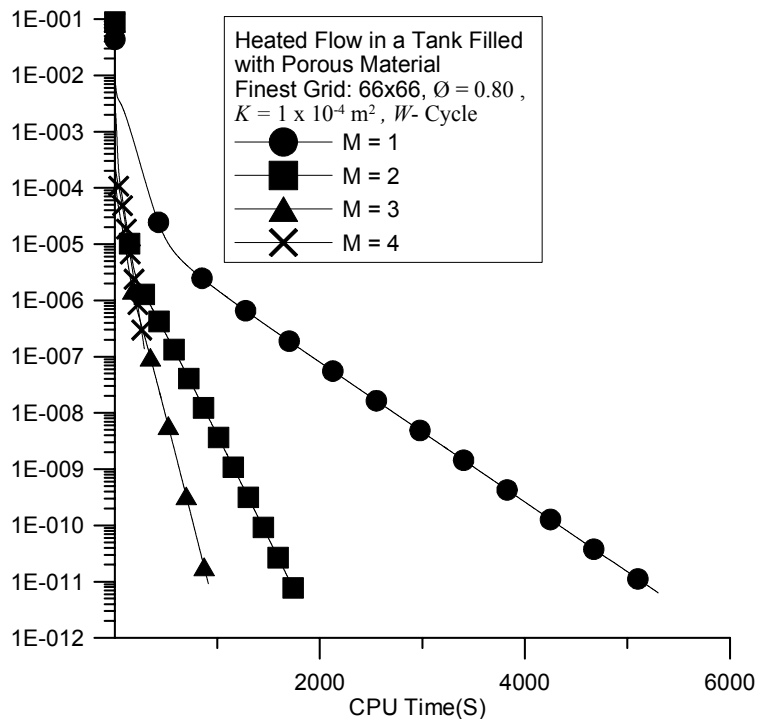


Figure 6 - Residue history for different number of grids, $Re_{in} = 300$, *W*-Cycle.

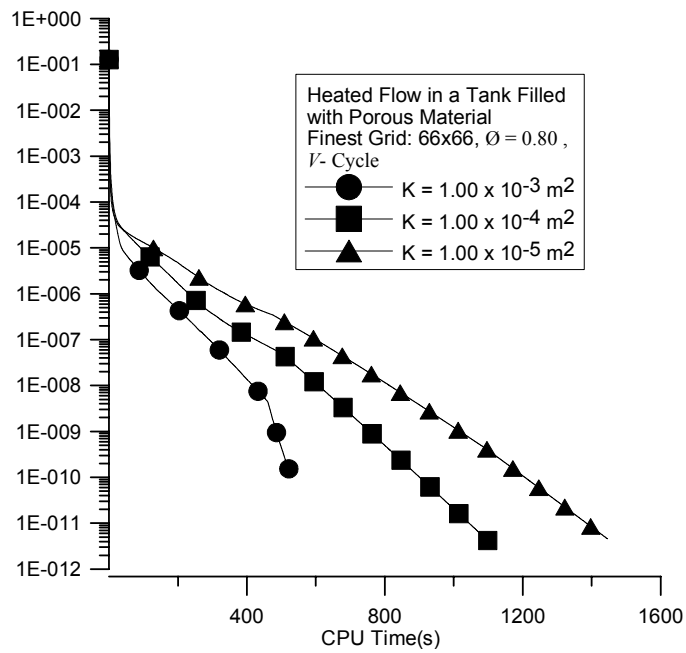


Figure 7 - Effect of Permeability K on residue history of Temperature T for 4-grids, $Re_{in} = 300$.

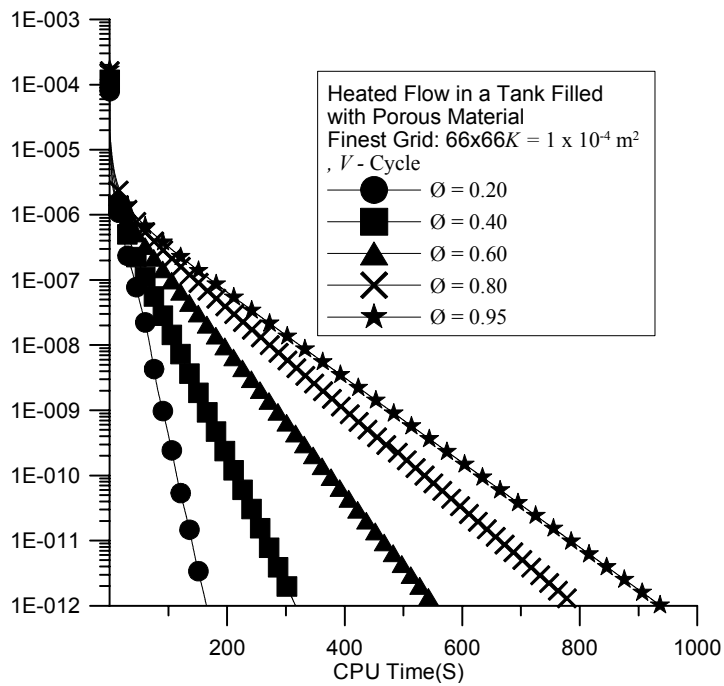


Figure 8 – Effect of Porosity ϕ on residue history of velocity U for 4-grids, $Re_{in} = 300$.

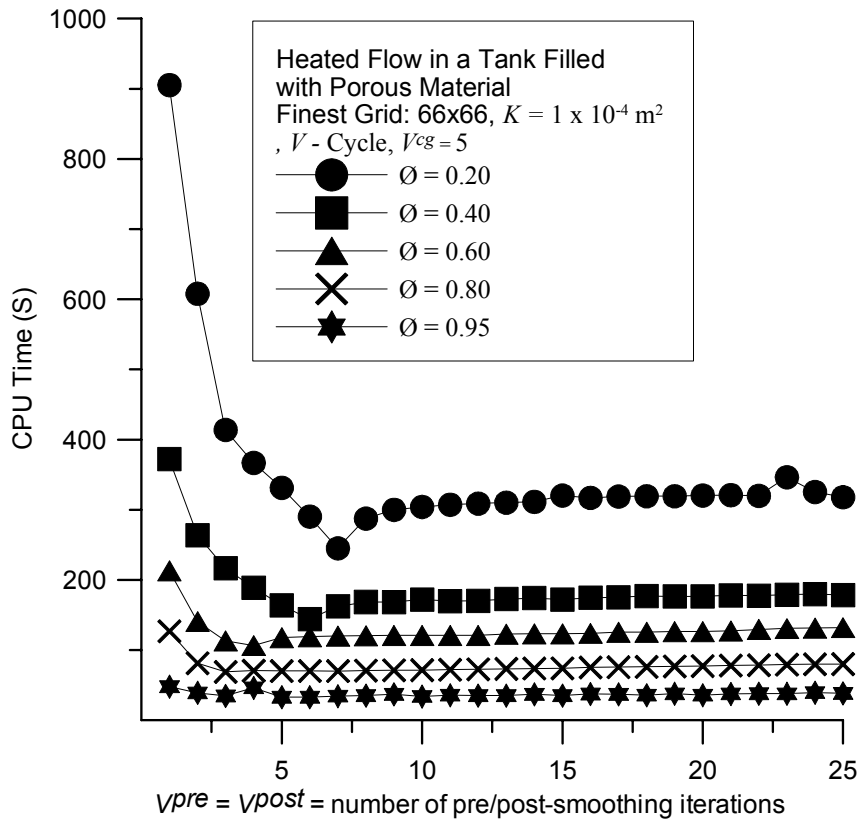


Figure 9 – Influence of the number of pre/post-smoothing iterations for differences porosities.

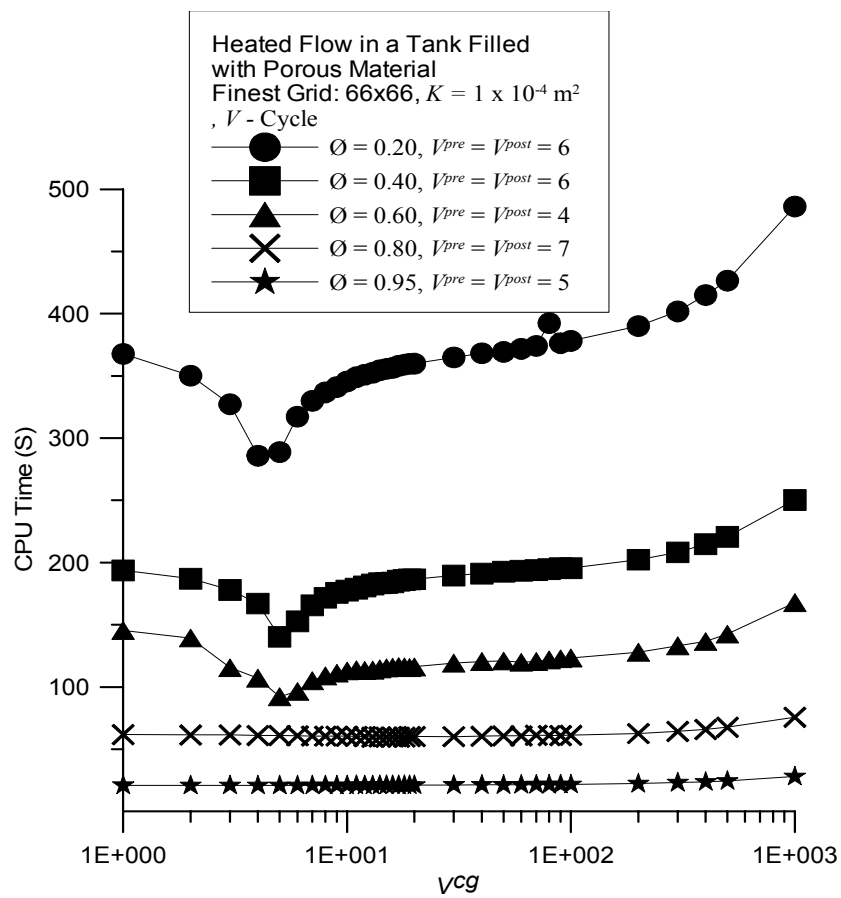


Figure 10 – Influence of the number of coarsest-grid iterations, v^{cg} , on the computational effort for differences numbers of porosities.